RSC Sustainability

ROYAL SOCIETY OF CHEMISTRY

PAPER

View Article Online
View Journal | View Issue

Cite this: *RSC Sustainability*, 2025, **3**, 1122

From citrus waste to value: optimizing sulfonated carbons for limonene upcycling into value-added products†

Gabrielle M. Reis, [a] Renan S. Nunes,[a] Gabriela T. M. Xavier,[a] Marina V. Kirillova,[b] Alexander M. Kirillov, [b] Dalmo Mandelli [a] and Wagner A. Carvalho *[a]

Limonene extracted from orange essential oil represents one of the globally prevalent and low-cost terpenes. Through the isomerization of limonene, it is possible to obtain a variety of high-added-value terpenic compounds such as terpinolene, α-terpinene, and γ-terpinene, as well as *p*-cymene. These products have diverse applications in the food, cosmetic, polymer, and chemical industries. The present study focused on developing a sustainable approach to producing valuable chemicals from renewable resources such as limonene, particularly *via* the isomerization of limonene over modified sulfonated carbons as bio-based catalysts. The synthesis of sulfonated carbons from glucose was optimized through a Central Composite Rotatable Design (CCRD), which enabled the identification of correlations between synthesis conditions and catalytic performance. Thus, sulfonated carbon catalysts with larger surface areas and smaller pore diameters lead to higher results in limonene isomerization. Various characterization techniques were employed to elucidate the physicochemical properties of the synthesized carbons, confirming the presence of acidic surface groups and showing the influence of textural characteristics on the limonene isomerization. After a 2 hour reaction at 150 °C, a 96% conversion of limonene was achieved, resulting in a good overall yield of the major products, ranging from 40% to 50%, namely α-terpinene, γ-terpinene, and terpinolene. The obtained findings highlight that the use of sulfonated carbons has the potential to drive the sustainable transformation of limonene into valuable compounds. In particular, the sustainability approach of this work includes (i) using a minimal amount of concentrated H_2SO_4 acid in the catalyst synthesis, (ii) employing bio-based and metal-free carbon catalysts, (iii) exploring a renewable substrate, and (iv) conducting the reaction process without added solvents.

Received 2nd July 2024
Accepted 11th December 2024

DOI: 10.1039/d4su00348a

rsc.li/rscsus

Sustainability spotlight

The study addresses the circular economy by utilizing limonene extracted from orange essential oil, a widely available and renewable resource. The use of sulfonated carbons synthesized from glucose underscores a commitment to bio-based materials. These catalysts are not only derived from renewable sources but also offer a metal-free alternative. Under optimized conditions, it was possible to achieve a 96% conversion of limonene with significant yields (40–50%) of valuable terpenic compounds (α-terpinene, γ-terpinene, terpinolene) demonstrating the effectiveness of the isomerization process. Furthermore, conducting the isomerization reaction without additional solvents not only decreases environmental impact but also cuts operational expenses. This approach promotes cleaner production methods and improves the economic feasibility of process scale up.

Introduction

The production of value-added chemicals from renewable carbon sources is crucial for a sustainable economy. Researchers are increasingly focusing on waste materials as sources of organic compounds to meet environmental protection goals. Essential oils are auspicious, offering both environmental and economic benefits.[1–3] As main components of many essential oils, terpenes represent an important class of bio-based substrates to produce a diverse range of compounds with significance for the chemical industry.[4] Orange essential oil,

[a]*Center for Natural and Human Sciences, Federal University of ABC (UFABC), Santo André, Brazil. E-mail: wagner.carvalho@ufabc.edu.br*

[b]*MINDlab: Molecular Design & Innovation Laboratory, Centro de Química Estrutural, Institute of Molecular Sciences, Departmento de Engenharia Química, Instituto Superior Técnico, Universidade de Lisboa, Lisboa, Portugal*

† Electronic supplementary information (ESI) available: Additional tables and figures detailing the preparation and characterization of the carbon catalyst, as well as catalytic activity studies (Tables S1–S3 and Fig. S1–S6), and data from control experiments (Fig. S7 and S8). See DOI: https://doi.org/10.1039/d4su00348a

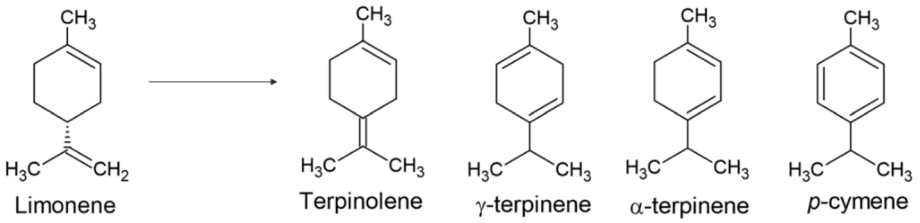

Fig. 1 Products obtained from the isomerization of limonene.

derived from orange peel and rich in limonene, represents a globally prevalent and low-cost terpene source.[5,6] Among the processes applicable to this terpene, limonene isomerization stands out, yielding a diverse range of high-value-added products such as terpinolene, α-terpinene, γ-terpinene, and *p*-cymene (Fig. 1).[7,8] These products find applications as additives in the food, cosmetics, and pharmaceutical industries. Most of these molecules also display antifungal and antibacterial properties.[9,10]

Catalysis plays a crucial role in converting and upcycling limonene into added-value products. However, many processes employ homogeneous catalysts, presenting challenges regarding their separation from the reaction medium, stability, and cost.[4] There are studies on the conversion of limonene using catalysts with metallic and acid sites, wherein the presence of Brønsted and Lewis acid sites might be competing. In almost all cases, terpenes, *p*-cymene, terpinolene, and other aromatic compounds are obtained.[11] A typically accepted mechanism for the transformation of limonene indicates the occurrence of several competitive reactions. These include isomerization, disproportionation, and polymerization catalyzed by Brønsted sites, while dehydrogenation may occur at Lewis sites.[9,12,13] For these reactions, increasing attention has been directed to the use of heterogeneous catalysts, such as carbon derivatives, given their low cost and production from agricultural or industrial waste, thus contributing to the circular economy.[7,14–16] These catalysts offer significant advantages, including their ability to form porous structures incorporating various active functional groups, such as carboxylic acid, hydroxyl, ketone, lactonic, and sulfonated groups. There are various techniques available to produce sulfonated carbons. Typically, a raw material undergoes carbonization *via* pyrolysis or hydrothermal processes, followed by an acidification step to anchor sulfonic groups.[17–19] As a common method, pyrolysis involves decomposing raw material in an inert atmosphere flux at temperatures exceeding 400 °C. During pyrolysis, oxygenated groups are reduced through decomposition, resulting in a hydrophobic surface, which can hamper the anchoring of acidic groups. Consequently, this process is costly as it requires multiple steps, high temperatures, and generates a substantial volume of gases.[20–26] Another process, known as hydrothermal carbonization (HTC), takes place in hot water at temperatures between 180–300 °C. This method offers several advantages over pyrolysis, including the ability to be conducted without the need to pre-dry the feedstock. Hence, HTC can yield carbons with high surface functionality that often contain oxygenated groups.[23,25,27,28] After the carbonization process and the production of carbon, this material can be acidified to anchor sulfonic groups, thereby forming a sulfonated carbon. Various sulfonation agents can be used, such as chlorosulfonic acid, concentrated or fuming H_2SO_4, organosulfonic acids (*p*-toluenesulfonic acid, hydroxyethylsulfonic acid and SO_3H-containing aryl diazonium derivatives).[17,29] Among these reagents, H_2SO_4 is the most used due to its low cost.[29]

Therefore, unlike methods involving pyrolysis or HTC followed by acidification, the process of hydrothermal carbonization assisted with H_2SO_4 (known as carbonization and *in situ* sulfonation), reduces time, energy, and reagent usage, making it a more cost-effective synthetic method.[30] In this method, sulfonic groups are incorporated into the biomass structure in a single step. The biomass is enclosed in a reactor, combined with H_2SO_4, and then heated to the desired temperature for a specific time. In contrast to the common HTC method, a sulfonated carbon with a high oxygen content on its surface is obtained, providing the material with hydrophobic interior and hydrophilic surface characteristics, which facilitate the incorporation of acidic groups.[31,32]

This study, aligned with the interest in producing bio-based carbon catalysts and functionalizing limonene as a feedstock, focused on synthesizing sulfonated carbons using the carbonization and *in situ* sulfonation methods. Multivariate Design of Experiments (DoE) was employed to optimize the concentration of H_2SO_4 and temperature. The resulting sulfonated carbons were then evaluated in limonene isomerization, aiming to produce products of significant importance to the chemical industry. The carbon-based catalysts were prepared by treating glucose with sulfuric acid under optimized conditions, including temperature, reaction time, and acid concentration. This study provides valuable insights into the impact of different variables on the synthesis of carbon catalysts and their activity, integrating both catalyst preparation and its performance in limonene conversion.

Materials and methods

Sulfonated carbons were synthesized using glucose obtained from LabSynth (Diadema – SP, Brazil). To carbonize and insert sulfonic groups onto the solid precursors, sulfuric acid (>98%) from LabSynth (Diadema-SP) was employed. The resulting solid materials were subsequently washed with acetone (>98%) from Cosmoquímica Indústria e Comércio (Barueri-SP). For studying the isomerization of limonene, the primary raw material was *R*-(+)-limonene from Sigma with a purity of 96%. During the gas chromatography (GC) analyses, reference standards were employed to ensure accuracy. These standards were acquired

Table 1 Central composite experimental design and responses studied[a]

	Factors		Responses						
Runs	x_1	x_2	y_1	y_2	y_3	y_4	y_5	y_6	y_7
1	0.9	97.6	4.9	2.3	56.3	1.6	1.5	0.9	8.0
2	2.6	97.6	5.2	2.2	9.3	0.03	0.1	0.02	0.4
3	0.9	182.4	4.8	1.6	94.1	20.5	3.6	11.2	17.9
4	2.6	182.4	6.5	2.5	68.6	6.6	2.5	4.03	18.7
5	0.5	140.0	4.7	1.7	71.0	11.0	1.6	6.6	22.9
6	3.0	140.0	5.7	2.4	23.9	2.5	0.9	1.4	7.6
7	1.7	80.0	5.5	2.2	16.4	0.1	0.4	0.09	0.9
8	1.7	200.0	6.4	2.2	87.5	12.9	0.9	4.4	7.9
9	1.7	140.0	5.6	1.9	97.7	27.1	4.4	11.4	17.1
10	1.7	140.0	4.9	2.9	99.0	22.0	6.5	7.4	13.4
11	1.7	140.0	4.8	2.6	99.0	15.7	8.0	5.4	9.7

[a] (x_1) mass of sulfuric acid for 1 g of glucose (g); (x_2) temperature (°C); (y_1) total acid groups (mmol g^{-1}), (y_2) sulfonic and carboxylic groups (mmol g^{-1}), (y_3) conversion of limonene (%), (y_4) α-terpinene yield (%); (y_5) *p*-cymene yield (%); (y_6) γ-terpinene yield (%); (y_7) terpinolene yield (%).

from Sigma Aldrich (purity indicated in %), including terpinolene (90%), α-terpinene (89%), γ-terpinene (97%), and *p*-cymene (99%). Decane was employed as an external standard (with a purity of 99%) to aid in the standard quantification.

Preparation of sulfonated carbons

The sulfonated carbon samples were generated through hydrothermal carbonization using concentrated sulfuric acid (HTC-H_2SO_4). The term HTC-H_2SO_4 is used to differentiate this method from traditional thermochemical processes such as pyrolysis, gasification, and hydrothermal carbonization. This process was conducted in a Teflon-lined stainless steel autoclave reactor with a total capacity of 80 mL. For each gram of glucose, a specific quantity of sulfuric acid was used, varying according to the designated mass of sulfuric acid for each run, denoted by the variable x_1 in Table 1. The system was hermetically sealed and immersed in an oil bath, maintaining the desired temperature for 6 h.

To complete the catalyst preparation, the reactor was slowly cooled to room temperature, and the carbon was washed with distilled water to remove any residual free acid present in the solid. Subsequently, the obtained carbons were washed using acetone within a Soxhlet apparatus to eliminate non-carbonized organic substances. The resulting solids were dried in an oven at 60 °C for 12 h, and then triturated to obtain a homogeneous powdered material.

Experimental design

The optimization of sulfonated carbon production was carried out using multivariate Design of Experiments (DoE). In these studies, Design Expert software (Stat-Ease Inc.) was used to create the experimental design, perform the analysis of variance (ANOVA), and adjust statistical models using Response Surface Methodology (RSM).

The experiments were performed using a Central Composite Design consisting of 11 runs, with an additional 3 replicates at the center point, as outlined in Table 1. The factors under investigation were temperature and the amount of H_2SO_4. The responses evaluated included surface acidity levels and the results from catalytic tests.

Characterization of sulfonated carbons

The quantification of acid groups was made using the Boehm Method (Boehm, 2002). A FE-SEM JMS-6701F JEOL instrument, operating at 10–15 kV, was utilized in the microscopy analysis coupled with Energy Dispersive Spectroscopy. Before analyses, the samples were coated with a 20 nm layer of gold using a Sputtering Leica EM ACE 200 instrument. Infrared spectra were acquired using a Varian-Agilent 640-IR FT-IR Spectrometer, with a resolution of 4 cm^{-1} and an accumulation of 16 scans (in ATR mode). Elemental analysis encompassing carbon, hydrogen, nitrogen, and sulfur was conducted on a Thermo Scientific Flash EA 1112 Elemental Analyzer, using tin capsules for sample containment.

For the N_2 sorption/desorption isotherms, measurements were conducted at 77 K using a Quantachrome Autosorb 1-MP instrument. efore analysis, the samples underwent a degassing process at 423 K for 24 h. The surface area was calculated using relative pressures ranging from 0.01 to 0.05 for all samples, following ISO 9277.

Catalytic isomerization of limonene

Limonene isomerization was carried out in 25 mL glass flasks equipped with a reflux condenser and subjected to magnetic stirring. The experimental conditions were adapted from the literature: temperature of 150 °C, 5 mL of limonene, and 15 wt% of catalyst, based on the initial mass of limonene.[1] Samples were withdrawn from the reaction at time intervals of 0.25, 0.5, 1, 2, and 4 h. To ensure accuracy, the catalysts were previously dried in an oven set at 60 °C for 12 h, to eliminate any potential humidity-related interference.

Subsequently, they were individually introduced into the glass flask, alongside the limonene. This setup was then connected to a reflux condenser and immersed in a preheated oil bath. The reaction time measurement began upon immersion in the oil bath.

The reaction products were analyzed using an Agilent GC 7890B device equipped with a FID detector and HP-5 capillary column of 30 m × 0.250 mm × 0.25 μm.

$$C\_\text{limonene} = \frac{(\text{limonene quantity at a given time} - \text{initial limonene quantity})}{\text{initial limonene quantity}} \times 100$$

The conversion (C_limonene) and product yield (y_i) were determined using the following equations.

$$y\_\mathrm{i} = \frac{(\text{product i quantity at a given time})}{\text{initial limonene quantity}} \times 100$$

Results and discussion

Optimization of *in situ* carbonization and sulfonation methodology

The synthesis of sulfonated carbons was optimized using the multivariate design of experiments. Catalytic responses, such as limonene conversion and yield of the isomerization products, were used to analyse and optimize the performance of the catalysts. On the other hand, characterization responses, such as the amount of acid groups, were employed to investigate the correlations between the properties of catalysts and their performance.

Table S1† presents the ANOVA results concerning all the responses investigated. A coefficient was considered statistically significant if its p-value was below or equal to 0.1 (90% confidence). This consideration arises from the inherent variability in processes such as material synthesis or catalysis. The statistical model was then refined to incorporate only the values above 90% confidence based on the p-value analysis.

Analysis of surface acid groups

The number of surface groups was used as one of the responses to optimize the carbonization and sulfonation method. Fig. S1† shows the amount of acid groups subdivided into (A) total acid groups and (B) carboxylic + sulfonic groups. The quantity of the latter remained consistent throughout the study, suggesting that neither of the two variables examined (amount of H_2SO_4 and carbonization temperature) influenced the quantity of these groups in the catalysts. For this reason, it was not possible to adjust an adequate model to this response.

Fig. 2 depicts the two variables used to evaluate the total amount of acidic groups. Based on this model and the regression results (Table S1†), the influence of the studied variables on the overall amount of acidic groups is evident, indicating a synergistic interaction between them.

It was observed that increasing the temperature and maintaining the amount of H_2SO_4 led to elevated levels of total acidic groups. However, the significant impact of temperature was only pronounced when combined with a higher H_2SO_4 concentration. In cases with a lower H_2SO_4 : glucose ratio, no notable increase in the total quantity of acidic groups was observed upon raising the temperature.

Furthermore, when the temperature is held constant and only the amount of H_2SO_4 is varied, an increase in the total amount of acidic groups is observed.

The *in situ* sulfonation process promotes the generation of a higher quantity of functional groups within the developing carbonaceous structure. Because of the less organized nature of the structure, the incorporation of acidic groups becomes more manageable. By keeping the functionalizing agent present during the carbonization of the precursor, it becomes possible to increase the number of functional groups formed throughout the structure, both on the surface and within the material's interior. As a result, the *in situ* functionalization method can provide a higher density of acidic groups on the carbon surface.

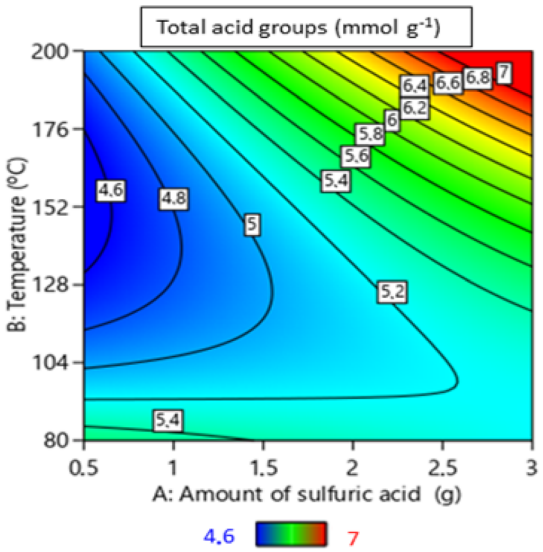

Fig. 2 Response surface obtained in the optimization process of sulfonated carbons through carbonization and *in situ* sulfonation. Effect of temperature and H_2SO_4 quantity on total acidic groups quantification.

A lower concentration of sulfuric acid reduces the availability of protons, which slows the reaction rate and limits the formation of acidic groups, even at higher temperatures. This underscores the crucial role of a sufficient supply of H^+ ions in catalyzing chemical reactions. Conversely, a higher sulfuric acid concentration creates a strongly acidic environment, which promotes efficient acid reactions, accelerates dehydration, and enhances bond cleavage. This results in an augmented formation of acidic groups during the carbonization, with temperature synergistically amplifying these effects. Thus, the increase in temperature in highly acidic environments has a favourable impact on the optimized formation of acid groups on the sulfonated carbon.

Analysis of catalytic performance in limonene isomerization

The catalytic performance of sulfonated carbons was experimentally evaluated in the limonene isomerization. Kinetic curves were obtained for each catalyst listed in Table 1 under the studied conditions (for details, see Fig. S2, ESI†). Control experiments were carried out without the catalyst, resulting in no formation of limonene isomerization products. In addition, further experiments were performed with different concentrations of sulfuric acid to simulate the partial or complete leaching of acidic groups from the catalyst. These experiments showed limonene conversion, but with significantly reduced

selectivity for the desired products, leading to the unwanted polymerization of the reaction products.

Continuous stirring was upheld throughout the reactions to ensure the optimal interaction between the catalyst's sites and substrate molecules. This method kept the catalyst particles suspended, minimizing any potential diffusion-related constraints. The resulting reaction mixture consisted primarily of isomerization products: α-terpinene, γ-terpinene, *p*-cymene, and terpinolene (Fig. S2†), alongside a non-volatile fraction identified as high molecular weight polymers. Although the study emphasizes a non-selective approach, it includes the entire spectrum of valuable terpenes obtained from limonene isomerization, rather than concentrating on a single compound. These limonene derivatives possess a number of industrial applications.

Specifically, both run 3 with a catalyst prepared with 0.9 g of H_2SO_4 at 182.4 °C, and the central point tests utilizing a catalyst prepared with 1.8 g of H_2SO_4 at 140 °C, demonstrated an impressive limonene conversion exceeding 90%. These specific tests show approximately 20%, 11%, and 17% yields of α-terpinene, γ-terpinene, and terpinolene, respectively. Retajczyk *et al.*[33] meticulously explored the mechanism of limonene isomerization, revealing the crucial involvement of Brønsted acid sites. In this process, consensus prevails regarding the adsorption of limonene molecules onto acidic sites *via* the exocyclic double bond, leading to a more stable tertiary carbenium ion. Subsequently, terpinolenes, terpinenes, and "polymeric species" are formed. A subsequent phase is accountable for generating *p*-cymene, with some evidence suggesting an involvement of Lewis acid[34] sites or even non-catalytic processes. The initiation of *p*-cymene production occurs through the oxidation of limonene isomerization products, a process further facilitated by the presence of O_2.[35] In all the reactions investigated in this study, the production of *p*-cymene was notably reduced, wherein neither Lewis acid sites nor O_2 were present in the reaction medium.

Furthermore, it is essential to consider the temperature of the reaction medium, as an increase in temperature tends to enhance limonene conversion but also leads to a higher generation of polymer byproduct.[36,37] Thus, according to the mechanism,[38] the process begins with a proton from an acidic site attaching to the exocyclic double bond of limonene, forming a carbocation. Subsequently, the removal of a proton leads to the formation of terpinolene.

Further double-bond isomerization can convert terpinolene into α-terpinene and terpinene, a process facilitated by additional acidic sites.

The *p*-cymene can also be formed from terpinenes with the assistance of Brønsted acid sites. Intermediates may also undergo dehydrogenation, requiring elevated temperatures to achieve satisfactory *p*-cymene yields.[39] This aspect will undergo a more comprehensive evaluation in subsequent sections of this study.

The response surfaces, shown in Fig. 3, were obtained with the reaction time kept constant at 2 h – duration during which most reactions were observed to reach equilibrium. The results from the Central Composite Rotatable Design (CCRD) methodology underscored considerable response variations across the experimental spectrum.

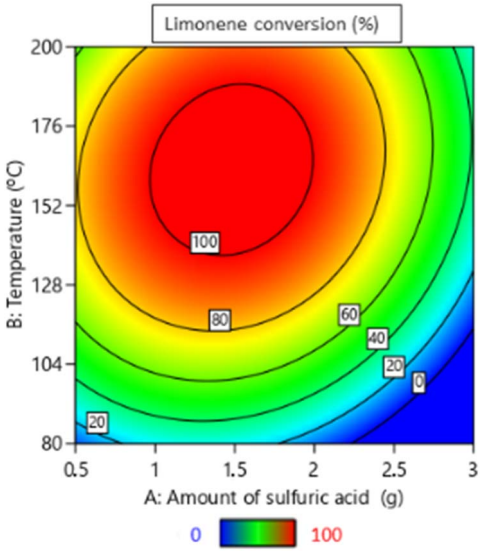

Fig. 3 Response surface obtained in the optimization process of sulfonated carbon catalysts through *in situ* carbonization and sulfonation. Effect of temperature and H_2SO_4 quantity on limonene conversion.

Statistical models were tailored to the experimental data. Through an analysis of variance (ANOVA), it was established with a 90% confidence that the models exhibit a significant regression while demonstrating a non-significant lack of fit, as can be seen in Table S1.†

The response surface shown in Fig. 3 for limonene conversion indicates that higher conversions were achieved when using a carbon catalyst prepared with lower quantities of H_2SO_4 and at higher temperatures. The same trend was obtained for the yields of products derived from limonene isomerization (Fig. 4).

This observation is significant as it suggests that reducing the amount of H_2SO_4 during catalyst preparation could yield a material that enables even higher limonene conversion. Connecting this data to Fig. 2, catalysts with a low total acidic group content can be obtained under these conditions – specifically, when using high quantities of H_2SO_4 and low temperatures during the catalyst preparation.

Surprisingly, this trend exhibits an inverse correlation between the total acidic groups with the conversion of limonene and/or the yield of limonene isomerization products. Hence, a tendency toward favorable product outcomes is evident when using catalysts prepared with low quantities of H_2SO_4.

These findings highlight an indirect correlation between the catalytic activity and total acid groups on the surface of sulfonated carbons. These catalytic materials, characterized by a solid structure with an oxygen-rich surface, are particularly interesting as they bear a hydrophobic core and a hydrophilic surface.

Notably, the carbon-based catalysts exhibit a remarkable ability to incorporate significant amounts of hydrophilic

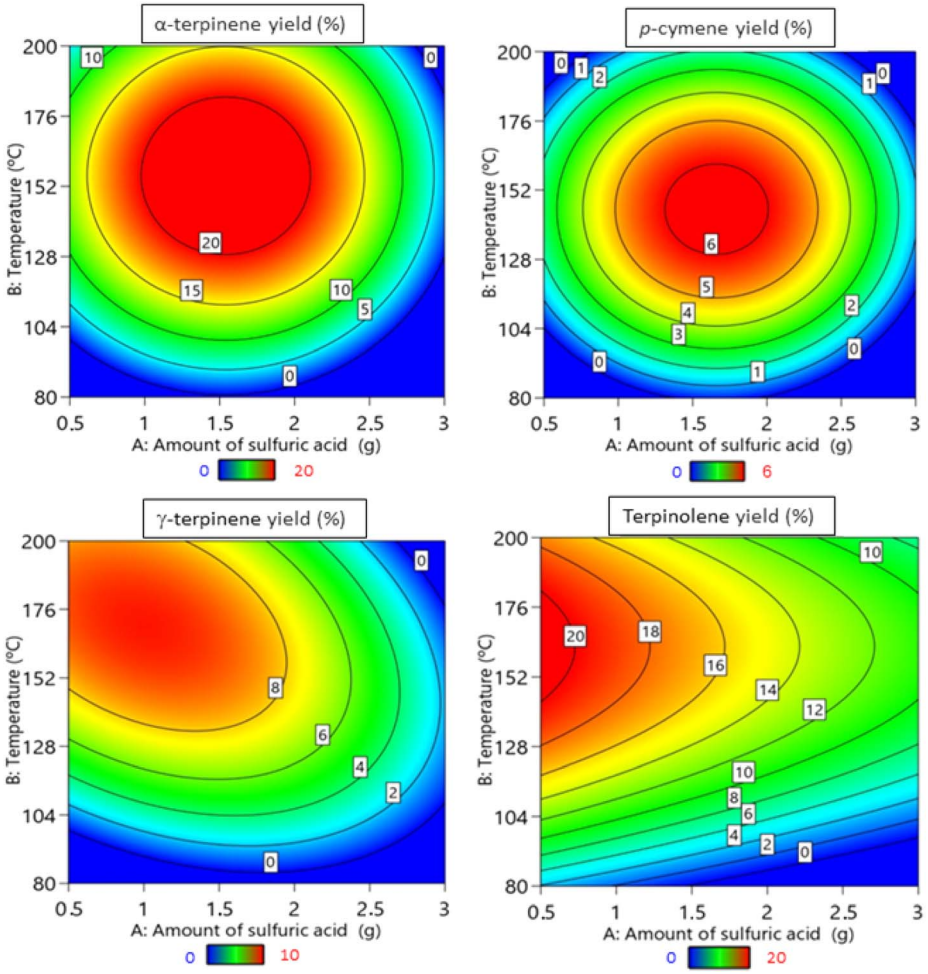

Fig. 4 Response surface obtained in the optimization process of sulfonated carbons through *in situ* carbonization and sulfonation. Effect of temperature and H_2SO_4 quantity during catalyst preparation on products of limonene isomerization.

molecules into their structures, which is facilitated by the presence of hydrophilic functional groups like SO_3H, COOH, and OH. In contrast, limonene is hydrophobic and demonstrates a low affinity for hydrophilic surfaces.[40,41] This hydrophobic nature of limonene may play a crucial role in specific catalytic reactions where interaction with hydrophilic surfaces might not be favored.[42,43]

Characterization

The methodology used in this study resulted in the formation of various oxygen-containing groups in the sulfonated carbons, such as lactone, phenolic carboxylic, and sulfonic groups. The presence of these functional groups can be confirmed by FTIR spectra (Fig. S3, ESI†). The bands at 1600, 1700, and 3400 cm^{-1} correspond to the stretching C=C, C=O, and O–H vibrations, respectively. Furthermore, the bands at 1043, 1173, and 1396 cm^{-1} indicate the presence of SO_3H groups.[44,45]

An analysis of the prepared carbon catalysts was carried out using scanning electron microscopy in combination with energy-dispersive X-ray techniques (Fig. S4, ESI†). The micrographs of the solids revealed particles with irregular geometries. Variations in morphologies were evident by the chosen synthesis conditions. The SEM micrographs from this study revealed particles with irregular geometries and surfaces, showing no well-defined crystalline grains. The materials exhibited a smooth or irregular surface with uniform contrast and irregular fracture patterns, supporting the presence of an amorphous structure.

Although there were slight variations in the micrographs, a common feature was evident across all catalysts – they exhibited amorphous structures with moderate levels of definition. This absence of structurally ordered particles can be ascribed to the *in situ* carbonization and sulfonation processes, which instigate a sequence of dehydration, oxidation, and precursor condensation reactions.

The chemical composition of the samples was determined using elemental analysis and energy-dispersive X-ray spectroscopy (Table S2, ESI†). From the results, a successful incorporation of sulfur into the carbon structure is evident. However, it is notable that even though the temperature effect is more substantial than the impact of H_2SO_4 quantity, this influence did not significantly affect the sulfur content (%). This result

aligns with the findings regarding carboxylic + sulfonic groups, where neither of the two variables impacted the presence of these groups in the catalysts.

The textural properties of the prepared sulfonated carbons are given in Table S3 (ESI†). The synthesis conditions employed had a direct impact on the textural properties of the materials. The specific surface area values, determined by the Brunauer–Emmet–Teller (BET) method, indicate that larger surface areas were obtained at higher temperatures and relatively low sulfuric acid contents.

The results demonstrated that both temperature and acid concentration significantly influence pore formation in carbon materials. Keeping the temperature constant while increasing sulfuric acid concentration led to a reduction in the surface area of glucose-derived materials. Conversely, raising the temperature, as seen in runs 1 and 3, caused a substantial increase in BET surface area, indicating that higher temperatures enhance porosity. However, increasing the acid concentration, as observed in runs 1 and 2, resulted in a sharp decrease in BET surface area, suggesting that high acid levels can degrade the material, leading to reduced porosity. This interaction is particularly evident in run 4, where the combination of elevated temperature and high acid concentration inhibited the temperature's positive effects. Several authors support these findings. For instance, Sheng *et al.*[46] emphasized that synthesis temperature is a critical factor in maximizing the surface area of carbon materials. The authors demonstrated that as temperature increases, the surface area tends to grow due to enhanced activation of the materials, leading to the formation of a more porous structure. Isahak *et al.*[47] Fernández *et al.*[48] and Yao *et al.*[49] highlights that carbons prepared through sulfuric acid dehydration can display significantly higher surface areas. Therefore, balancing these parameters is crucial to optimizing pore formation and maintaining the structural integrity of the materials.

The correlation between textural properties and catalytic performance indicates that the sulfonated carbon catalysts with larger surface areas lead to superior results in limonene isomerization than those with smaller surface areas. This can be confirmed by examining the data in Table S3 (ESI†), wherein runs 2, 6, and 7 had the lowest surface area values (1.3, 2.7, 2.4 $m^2\ g^{-1}$, respectively) and exhibited modest catalytic activity. In contrast, experiments 3, 8, 9, 10, and 11 correspond to samples with the highest surface area values (109.5, 133.2, 74.1, 51.4, and 86.9 $m^2\ g^{-1}$, respectively). These catalysts lead to almost complete conversion of limonene within 2 h of reaction at 150 °C. Considering the optimization of limonene conversion (Fig. 3), it can be inferred that decreasing the amount of sulfuric acid and increasing the temperature during the synthesis of sulfonated carbons resulted in more effective catalysts for limonene isomerization.

These observations can be confirmed through the Heat Map Pearson's Correlation Analysis (Fig. S5, ESI†). The Pearson correlation is a statistical measure that assesses the linear relationship between two variables. The correlations were examined between the total number of acidic groups (y_1), the quantity of carboxylic and sulfonic groups (y_2), catalytic results (y_{3-7}), and textural properties (y_{8-10}).[50]

Based on the Pearson correlation matrix heat map presented in Fig. S5,† the analysis revealed important correlations among the variables, providing significant insights into the influence of textural properties on the limonene conversion and the yields of resulting products. A positive correlation was observed between the limonene conversion (y_3) and the yields of αterpinene (y_4), *p*-cymene (y_5), γ-terpinene (y_6), and terpinolene (y_7) with BET surface area (y_8), total pore volume (y_9), and micropore volume (y_{10}). This finding suggests that an increase in specific surface area (y_8) and pore volumes (y_9 and y_{10}) is associated with improved limonene conversion (y_3) and yields of these compounds. This relationship can be explained by the increased availability of active sites on the catalyst and greater accessibility to these sites, which facilitates reagent adsorption and catalytic reactions. Additionally, the analysis revealed a strong positive correlation between BET surface area (y_8) and micropore volume (y_{10}), indicating that an increase in surface area (y_8) is frequently associated with an increase in micropore volume (y_{10}). There was also a positive correlation between total pore volume (y_9) and BET surface area (y_8),suggesting that an increase in surface area (y_8) can be related to an increase in total pore volume (y_9). These results indicate that a modification of surface area (y_8) and pore volume (y_9 and y_{10}) can represent an effective strategy to enhance the textural properties of catalysts. In terms of catalytic activity, the positive correlations between textural properties and limonene conversion (y_3) and product yields (y_4, y_5, y_6, y_7) suggest that the optimization of surface area (y_8) and pore volumes (y_9 and y_{10}) might be crucial for improving catalytic performance. Higher BET surface areas (y_8) and micropore volumes (y_{10}) indicate the presence of more accessible active sites, facilitating limonene conversion reactions (y_3) and leading to superior yields of the desired compounds (y_4, y_5, y_6, y_7). These findings underscore the importance of textural properties, such as BET surface area (y_8), total pore volume (y_9), and micropore volume (y_{10}), in determining the catalytic efficiency and product yields in limonene conversion processes, providing a basis for developing strategies to optimize catalysts for maximizing catalytic efficiency.

A comparable result was obtained by Gu *et al.*,[51] who studied the enantioselective adsorption of limonene molecules by metal–organic frameworks (MOFs). They found that when the pore sizes are well-matched, approximately equivalent to the size of the adsorbed molecule, the stereogenic center has the greatest impact on the molecule, resulting in higher enantiomeric separation. Drawing parallels between the study conducted by Gu *et al.*[51] and the outcomes of the present work, it could be inferred that there is an optimal range of textural properties that promote the adsorption of limonene molecules. Overall, this study revealed that catalysts possessing more refined textural properties, particularly those with larger surface areas, yielded enhanced results in the isomerization of limonene.

Table 2 Optimization criteria used in the desirability method

Variable or response		Goal	Lower limit	Upper limit
(x_1) Sulfuric acid amount	(g)	None	0.5	3
(x_2) temperature	(°C)	None	80	200
(y_1) total acid groups	(mmol g^{-1})	None	4.7	6.5
(y_2) sulfonic and carboxyl groups	(mmol g^{-1})	Not used	1.6	2.9
(y_3) conversion of limonene	(%)	Maximize	9.3	99.05
(y_4) α-terpinene yield	(%)	Maximize	0.03	27.1
(y_5) *p*-cymene yield	(%)	Maximize	0.1	7.8
(y_6) γ-terpinene yield	(%)	Maximize	0.02	11.4
(y_7) terpinolene yield	(%)	Maximize	0.4	22.9

Definition of optimized synthesis conditions

As previously mentioned, statistical models were created to evaluate the catalytic efficiency and key physical and chemical properties of the sulfonated carbons. Employing these models, it was possible to fine-tune the *in situ* carbonization and sulfonation process to fulfill the predetermined objectives outlined in Table 2. The optimization criteria primarily aimed at maximizing the limonene conversion and enhancing the yields of α-terpinene, γ-terpinene, *p*-cymene, and terpinolene.

The optimum parameters were identified using the Desirability Function Method, a technique that converts individual variables and responses into a new mathematical construct termed the desirability function. This method assigns an overall desirability score ranging from 0 to 1, where a score of 1 signifies the achievement of the optimization criteria for all individual responses.[52] These criteria (Table 2) were established to optimize the limonene conversion and product yields regardless of the synthesis conditions of the carbon catalyst. The optimization procedure was performed utilizing Design Expert 13 software, resulting in a contour plot with comprehensive desirability (Fig. S6, ESI†). The optimum conditions involved the synthesis of the catalyst using 1.4 g of H_2SO_4 and a temperature of 155 °C, with an overall desirability of 0.83. The global desirability function reached its maximum value near the central point, which aligns with the optimized conditions.

Table 3 below illustrates the catalytic outcomes after a 2 h limonene isomerization utilizing the optimized sulfonated carbon catalyst. This table displays the modelled response results, the correlation coefficient (R^2), and the actual results for the optimized sulfonated carbon across several responses, which were adjusted to achieve the optimal synthesis conditions. This optimization was conducted based on responses amenable to modelling. To validate the optimization model for the sulfonated carbon and confirm its accuracy, confirmation tests, referred to as current responses, were conducted. Fig. 5 shows the kinetic graph of the catalytic activity of the optimized carbon catalyst. The obtained overall desirability function (0.827) and correlation coefficient values (R^2; Table S1†) suggest that the modelled responses satisfactorily predict the ideal

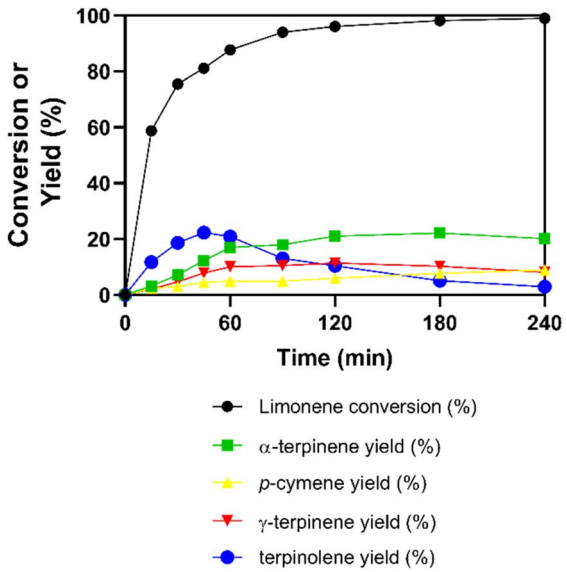

Fig. 5 Catalytic outcomes of limonene isomerization using the optimized sulfonated carbon catalyst (catalyst sample produced using 1.4 g of H_2SO_4 and a temperature of 155 °C). The experimental setup involved the utilization of 30 mmol of limonene, a catalyst loading of 15% by weight, and a reaction temperature of 150 °C.

Table 3 Experimental and predicted properties for the optimized sulfonated carbon from the CCRD

Variable or response		Model prediction	R^2	Obtained results
(y_1) total acid groups	(mmol g^{-1})	5.0 ± 0.3	0.88	6.0
(y_3) conversion of limonene	(%)	107 ± 4.8	0.99	96.0
(y_4) α-terpinene yield	(%)	23.0 ± 4.3	0.88	21.0
(y_5) *p*-cymene yield	(%)	6.0 ± 2.8	0.85	6.0
(y_6) γ-terpinene yield	(%)	9.0 ± 2.4	0.76	11.0
(y_7) terpinolene yield	(%)	17.0 ± 4.3	0.82	10.5
Desirability	—	0.83	—	—

Table 4 Comparison of limonene isomerization results using solvent-free systems from the literature

Catalyst	Time (min)	Catalyst amount (%)	Temperature (°C)	Conversion of limonene (%)	Product yields				References
					α-Terpinene (%)	γ-Terpinene (%)	Terpinolene (%)	*p*-cymene (%)	
Ti-SBA-15	120	10	150	32	11	2	17	0.5	38
Clinoptilolite	120	15	155	27	2	3	18	1.8	53
MS-1	180	15	160	95	18	15	5	10	36
Ti-SBA-16	120	15	150	30	5	2	16	2	54
Ti-MCM-41	120	15	170	60	15	6	19	3	55
Optimized sulfonated carbon	120	15	150	96	21	11	10.5	6	This work

system. In addition, the experimentally obtained results match the model predictions, thus validating the empirical model used.

Model simplifications, unaccounted variables, and experimental errors contribute to the differences between the predicted and actual outcomes in the catalytic system. Factors within the system prevent the R^2 value from reaching 1. Despite this, the developed model effectively predicts response behaviours, highlighting the complexity and experimental variability of the system. The optimization of the carbonization and sulfonation method, using varying temperatures and sulfuric acid quantities, demonstrates an interesting entry to the preparation of sulfonated carbon catalysts from bio-based raw materials.

Finally, selecting an optimal catalytic system can significantly enhance the efficiency of limonene isomerization, reduce production costs, and improve the overall sustainability of the process, enabling the upcycling of limonene into high-value-added products. The optimized catalyst developed in this study demonstrated exceptional performance, achieving a 96% conversion of limonene with notable product yields: 21% α-terpinene, 6% *p*-cymene, 11% γ-terpinene, and 10.5% terpinolene. As shown in Table 4, these results were compared to previous studies under similar conditions. It is evident that the catalyst produced in this work not only exhibited comparable or superior conversion rates and product yields, but also benefited from a more economical synthesis process and milder reaction conditions. This presents a clear competitive edge over other catalysts in the literature, which often require higher temperatures or more expensive materials.

In summary, this catalyst offers high yields of the desired products while standing out for its ease of production, low cost, and efficiency under moderate conditions. This makes it a promising and cost-effective alternative to conventional catalysts.

Recycling test

The stability and recyclability of the optimized sulfonated carbon catalysts were explored through successive catalytic runs. This investigation entailed subjecting the material to consecutive cycles, as depicted in Fig. 6.

The optimized sulfonated carbon catalysts showed a sharp decline in efficiency over successive cycles. Limonene conversion dropped from 96% in the first cycle to 33% in the fourth one, while the yield of terpinolene decreased by 8%. This decline is due to a build-up of residue that blocks pores and hinders an access to active sites. Despite these issues, the catalyst, prepared under mild conditions, performed well in initial cycles. It thus can be used in sustainable biomass conversion.

In our previous study[56] on sulfonated carbon for carbohydrate dehydration, a decline in catalytic performance across successive cycles was observed, primarily due to pore blockage that limits access to active sites. Catalysts with significant internal porosity are particularly affected, as many active sites reside within the pores, leading to increased mass transfer resistance and limited diffusion. This behavior is evident in glucose-derived carbon catalysts, underscoring the critical roles of surface area, porosity, and diffusional limitations in catalyst design.

Similarly, in biomass conversion, the formation of humins – complex organic polymers produced under high temperatures and acidic conditions – blocks active sites and reduces reaction efficiency.[57–64] This challenge also appears in terpene isomerization, where reactive intermediates such as carbocations polymerize into oligomers, causing further pore blockage.[36,37,65] Both humins and oligomers arise from similar polymerization mechanisms, which hinder catalytic performance. These issues highlight the importance of controlling reaction conditions to minimize byproduct formation and enhance catalytic efficiency across various chemical processes.

As previously shown by Gu *et al.*,[51] aligning pore sizes with the dimensions of the adsorbed molecule improved enantiomeric separation, particularly influenced by the stereogenic center. This study's findings confirm that as pores become clogged due to the accumulation of reaction residues over time, accessibility to active sites within the catalyst diminishes, consequently impairing catalytic efficiency. This pore blockage hinders the reaction at the stereogenic center, thus impeding the isomerization of limonene.

Another study that supports the findings presented in this research is that of He *et al.*[66] The authors investigated the

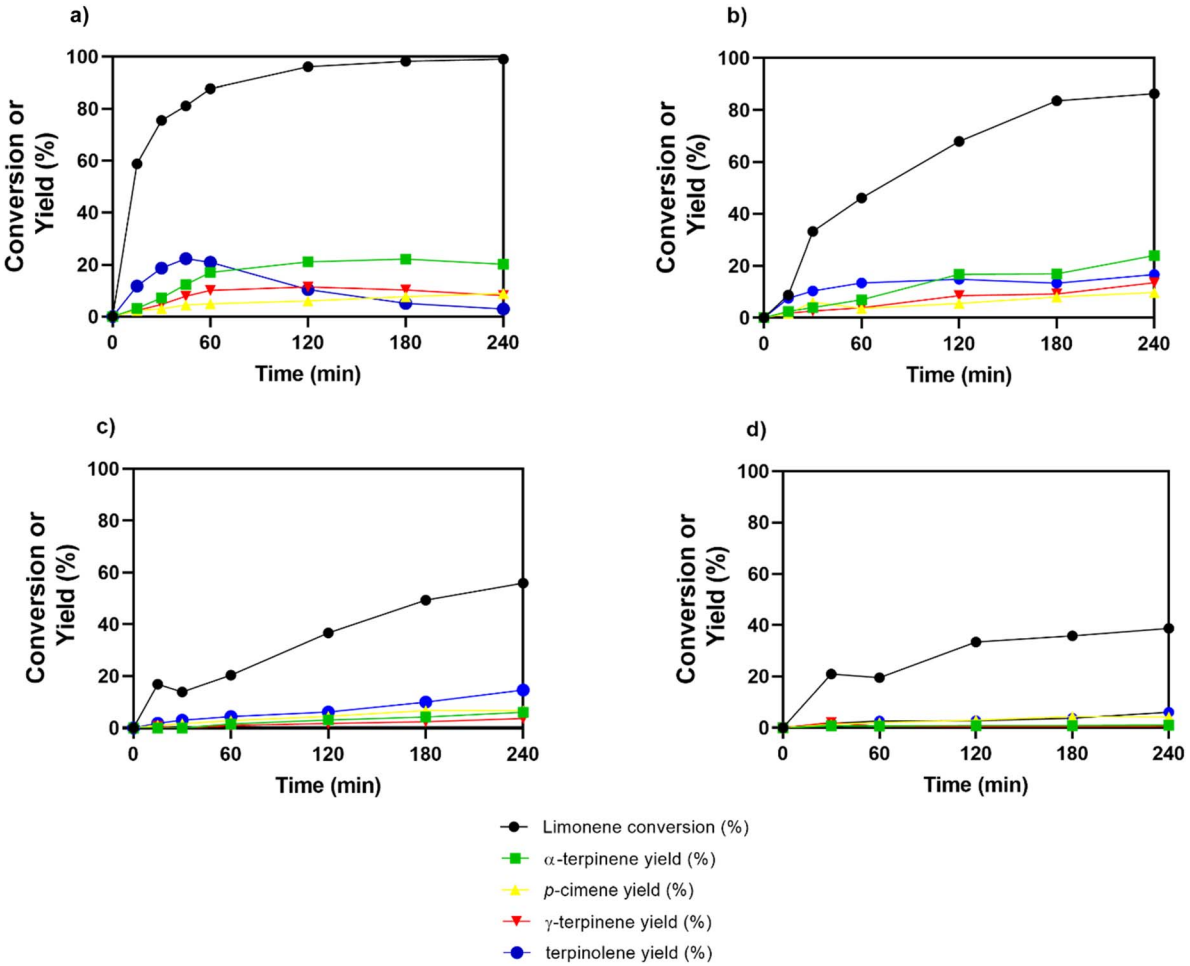

Fig. 6 Recycling test outcomes of limonene isomerization on the optimized sulfonated carbons (catalyst sample produced using 1.4 g of H_2SO_4 and a temperature of 155 °C. The experimental setup involved the utilization of 30 mmol of limonene, a catalyst loading of 15% by weight, and a reaction temperature of 150 °C. (a) First cycle, (b) second cycle, (c) third cycle, (d) fourth cycle.

isomerization of limonene using Metal-Macrocycle Frameworks (MMFs) as catalysts. They found that these porous structures offer a confined environment that suppresses secondary reactions, enabling the desired selectivity in terpinolene formation. Small pores enhance selectivity by restricting the access of larger molecules and facilitating selective interaction between substrates and desired products. In turn, larger pores may yield a broader range of products due to increased molecular mobility. However, small pores can hinder the reaction by limiting the access of reactant molecules to active sites, thus compromising the efficiency of isomerization. The acidity concentrated in specific pores provides additional catalytic sites, directing isomerization in a controlled manner and contributing to the selectivity observed in the process. Therefore, achieving a balance in pore size is crucial to ensure effective and selective interactions between reactant molecules, while preserving a controlled environment for the reaction.

Hence, the significance of the catalyst's pore structure and its impact on limonene isomerization is underscored by the findings presented in this study. The catalysts investigated herein feature a higher surface area, which, contrary to expectation, does not promote the selective formation of terpinolene. Instead, it generates additional products such as γ- and α-terpinene, alongside minor quantities of *p*-cymene.

Conclusions

The *in situ* carbonization and sulfonation process displayed promising potential in generating sulfonated carbons with Brønsted acid characteristics from a bio-based feedstock (glucose). Guided by the CCRD, the strategic planning allowed an in-depth assessment of the influence of variables on the preparation of the catalyst, demonstrating the synergistic effect between temperature and proton concentration on the formation of surface acid groups on carbon, especially sulfonic groups. Control experiments conducted without the catalyst showed no limonene isomerization. In contrast, experiments with free sulfuric acid led to reduced selectivity for isomerization products and considerable limonene polymerization. However, the acid catalysts exhibited remarkable activity in the limonene isomerization reaction, achieving over 90% conversion with a satisfactory overall product yield. The main primary products obtained comprise α-terpinene, γ-terpinene, *p*-cymene, and terpinolene, along with a non-volatile fraction composed of high molecular

weight polymers. The significant limitation in *p*-cymene production was attributed to the absence of Lewis acid sites and O_2 in the system. Analysis through CCRD unveiled the substantial influence of textural properties on limonene isomerization. The optimized conditions for the quantity of H_2SO_4 and temperature during the synthesis of sulfonated carbons were identified, suggesting the possibility of reducing energy and H_2SO_4 consumption for a more cost-effective catalyst production. The mild conditions of the *in situ* carbonization and sulfonation process, characterized by short reaction times and low glucose-to-sulfuric acid ratios, yielded sulfonated carbons with distinct Brønsted acid characteristics.

The Pearson correlation analysis revealed that a larger BET surface area positively correlates with increased yields of α-terpinene, *p*-cymene, γ-terpinene, and terpinolene, as well as greater micropore volume. This suggests that larger surface areas enhance catalytic activity by providing more accessible active sites, which improve limonene conversion and the yields of these products. Conversely, larger total pore volumes are positively correlated with the BET surface area, indicating that increases in the surface area are often associated with higher total pore volumes. This relationship highlights the importance of optimizing textural properties for effective catalysis. The analysis also suggests that modifying the BET surface area and pore volumes could be a key strategy to enhance catalytic performance.

The optimized sulfonated carbon catalysts demonstrated a significant decline in efficiency over four consecutive recycling cycles, with limonene conversion dropping from 96% in the first cycle to 33% in the fourth one, while the yield of terpinolene declined by 8%. This decrease was attributed to the blockage of pores, hindering access to active sites. Despite the very good initial performance, the gradual reduction in catalytic activity suggests that lowering the amount of sulfuric acid used in catalyst preparation could potentially provide catalysts with enhanced limonene conversion.

The obtained herein research findings highlight the significant potential of sulfonated carbon catalysts in facilitating the sustainable conversion of limonene into valuable compounds. Notably, the sustainability approach of this study involves (i) the utilization of bio-based and metal-free carbon catalysts, (ii) the use of an abundant and renewable substrate (limonene), and (iii) conducting the reaction process without the addition of a solvent. This work holds particular importance in advancing the development of future carbon-based sustainable catalysts and catalytic processes for the conversion of other terpenes and related biofeedstocks.

Data availability

The data supporting this article have been included as part of the ESI.† Fig. 2–4 were generated from the data presented in Table 1, utilizing Design Expert software version 13.

Author contributions

Gabrielle Mathias Reis: conceptualization, visualization, writing – original draft preparation. Renan S. Nunes: characterization, methodology. Gabriela T. M. Xavier: characterization, methodology. Marina V. Kirillova: conceptualization, methodology, resources. Alexander M. Kirillov: conceptualization, methodology, resources, writing – review & editing. Dalmo Mandelli: conceptualization, methodology, resources, review. Wagner A. Carvalho: supervision, conceptualization, methodology, resources, writing – review & editing.

Conflicts of interest

The authors declare that they have no known competing financial interests or personal relationships that could have appeared to influence the work reported in this paper.

Acknowledgements

This research was supported by the Human Resources Program of the National Agency of Petroleum. Natural Gas and Biofuels – PRH-ANP, supported with resources from the investment of oil companies qualified in the P. D & I Clause of ANP Resolution 50/2015. The authors also acknowledge the experimental support of the Multi-User Central Facilities (CEM/UFABC). This study was financed in part by the Coordenação de Aperfeiçoamento de Pessoal de Nível Superior – Brazil (CAPES) – Finance Code 001, Conselho Nacional de Desenvolvimento Científico e Tecnológico (CNPq – Brasil) (grant number 303658/2020-7), CAPES Print (grant number 8887.716150/2022-00) and Fundação de Amparo à Pesquisa do Estado de São Paulo (grant number 2018/01258-5, 2021/06471-1, 2021/12342-0, 2023/13334-6, and 2023/01634-5). AMK and MVK acknowledge the support from the Foundation for Science and Technology (FCT), projects: PTDC/QUI-QIN/3898/2020, UIDB/00100/2020, and LA/P/0056/2020.

Notes and references

1 M. Retajczyk, A. Wróblewska, Z. C. Koren, B. Michalkiewicz, A. Szymańska and P. Miadlicki, Synthesis, Characterization, and Catalytic Applications of the Ti-Sba-16 Porous Material in the Selective and Green Isomerizations of Limonene and s-Carvone, *Catalysts*, 2020, **10**(12), 1–17, DOI: **10.3390/catal10121452**.

2 J. H. Advani, A. S. Singh, N. H. Khan, H. C. Bajaj and A. V. Biradar, Black yet Green: Sulfonic Acid Functionalized Carbon as an Efficient Catalyst for Highly Selective Isomerization of α-Pinene Oxide to Trans-Carveol, *Appl. Catal., B*, 2020, **268**, 118456, DOI: **10.1016/j.apcatb.2019.118456**.

3 M. Nambiraj and K. Suresh Kumar, Impact of Essential Oils from Agro Waste as Antioxidants on Biodiesel Long-Term Storage Stability for CI Engines: Fresh and Aged Evaluations, *Process Saf. Environ. Prot.*, 2024, **186**, 1214–1228, DOI: **10.1016/j.psep.2024.04.087**.

4 V. V. Costa, K. A. Da Silva Rocha, I. V. Kozhevnikov, E. F. Kozhevnikova and E. V. Gusevskaya, Heteropoly Acid Catalysts for the Synthesis of Fragrance Compounds from Biorenewables: Isomerization of Limonene Oxide, *Catal. Sci. Technol.*, 2013, **3**(1), 244–250, DOI: **10.1039/c2cy20526b**.

5 Trademap, *Trade map - Trade statistics for international business development int. Trade Cent*, 2023, https://www.trademap.org/Country_SelProduct_TS.aspx?nvpm=1%7C%7C%7C%7C%7C3301%7C%7C%7C4%7C1%7C1%7C2%7C2%7C1%7C2%7C3%7C1%7C1.

6 D. Shaw, A. D. Tripathi, V. Paul, A. Agarwal, P. K. Mishra and M. Kumar, Valorization of Essential Oils from Citrus Peel Powder Using Hydro-Distillation, *Sustainable Chem. Pharm.*, 2023, **32**, 101036, DOI: 10.1016/j.scp.2023.101036.

7 C. Antonetti, M. Melloni, D. Licursi, S. Fulignati, E. Ribechini, S. Rivas, J. C. Parajó, F. Cavani and A. M. Raspolli Galletti, Microwave-Assisted Dehydration of Fructose and Inulin to HMF Catalyzed by Niobium and Zirconium Phosphate Catalysts, *Appl. Catal., B*, 2017, **206**, 364–377, DOI: 10.1016/j.apcatb.2017.01.056.

8 W. He, S. Tashiro and M. Shionoya, Highly Selective Acid-Catalyzed Olefin Isomerization of Limonene to Terpinolene by Kinetic Suppression of Overreactions in a Confined Space of Porous Metal-Macrocycle Frameworks, *Chem. Sci.*, 2022, **13**(30), 8752–8758, DOI: 10.1039/d2sc01561g.

9 M. Retajczyk and A. Wróblewska, The Isomerization of Limonene over the Ti-SBA-15 Catalyst—the Influence of Reaction Time, Temperature, and Catalyst Content, *Catalysts*, 2017, **7**(9), 273.

10 N. S. V. Lakshmayya, A. K. Mishra, Y. K. Mohanta, J. Panda, B. Naik, B. Mishra and R. S. Varma, Essential Oils-Based Nano-Emulsion System for Food Safety and Preservation: Current Status and Future Prospects, *Biocatal. Agric. Biotechnol.*, 2023, **53**, 102897, DOI: 10.1016/j.bcab.2023.102897.

11 S. Lycourghiotis, D. Makarouni, E. Kordouli, K. Bourikas, C. Kordulis and V. Dourtoglou, Activation of Natural Mordenite by Various Acids: Characterization and Evaluation in the Transformation of Limonene into p-Cymene, *Mol. Catal.*, 2018, **450**, 95–103, DOI: 10.1016/j.mcat.2018.03.013.

12 M. A. Martin-Luengo, M. Yates, E. S. Rojo, D. Huerta Arribas, D. Aguilar and E. Ruiz Hitzky, Sustainable P-Cymene and Hydrogen from Limonene, *Appl. Catal., A*, 2010, **387**(1–2), 141–146, DOI: 10.1016/J.APCATA.2010.08.016.

13 D. Makarouni, S. Lycourghiotis, E. Kordouli, K. Bourikas, C. Kordulis and V. Dourtoglou, Transformation of Limonene into P-Cymene over Acid Activated Natural Mordenite Utilizing Atmospheric Oxygen as a Green Oxidant: A Novel Mechanism, *Appl. Catal., B*, 2018, **224**, 740–750, DOI: 10.1016/J.APCATB.2017.11.006.

14 N. E. Leadbeater, *Organic Synthesis Using Microwave Heating*, Elsevier Ltd, 2014, vol. 9, DOI: 10.1016/B978-0-08-097742-3.00920-4.

15 M. Heidari, A. Dutta, B. Acharya and S. Mahmud, A Review of the Current Knowledge and Challenges of Hydrothermal Carbonization for Biomass Conversion, *J. Energy Inst.*, 2019, **92**(6), 1779–1799, DOI: 10.1016/j.joei.2018.12.003.

16 R. A. Sheldon, Green Chemistry, Catalysis and Valorization of Waste Biomass, *J. Mol. Catal. A:Chem.*, 2016, **422**, 3–12, DOI: 10.1016/j.molcata.2016.01.013.

17 T. Zhang, H. Wei, J. Gao, S. Chen, Y. Jin, C. Deng, S. Wu, H. Xiao and W. Li, Synthesis of Sulfonated Hierarchical Carbons and Theirs Application on the Production of Furfural from Wheat Straw, *Mol. Catal.*, 2022, **517**, 112034.

18 R. S. Nunes, T. C. Tudino, L. M. Vieira, D. Mandelli and W. A. Carvalho, Rational Production of Highly Acidic Sulfonated Carbons from Kraft Lignins Employing a Fractionation Process Combined with Acid-Assisted Hydrothermal Carbonization, *Bioresour. Technol.*, 2020, **303**, 122882, DOI: 10.1016/j.biortech.2020.122882.

19 Z. Zailan, M. Tahir, M. Jusoh and Z. Y. Zakaria, A Review of Sulfonic Group Bearing Porous Carbon Catalyst for Biodiesel Production, *Renewable Energy*, 2021, 430–452, DOI: 10.1016/j.renene.2021.05.030.

20 R. K. Srivastava, N. P. Shetti, K. R. Reddy, M. N. Nadagouda, M. Badawi, A. Bonilla-Petriciolet and T. M. Aminabhavi, Valorization of Biowastes for Clean Energy Production, Environmental Depollution and Soil Fertility, *J. Environ. Manage.*, 2023, 117410.

21 N. H. Zerin, M. G. Rasul, M. I. Jahirul and A. S. M. Sayem, End-of-Life Tyre Conversion to Energy: A Review on Pyrolysis and Activated Carbon Production Processes and Their Challenges, *Sci. Total Environ.*, 2023, **905**, 166981, DOI: 10.1016/j.scitotenv.2023.166981.

22 Y. Sun, C. Li, M. Fan, L. Zhang, S. Zhang, G. Hu and X. Hu, Distinct Nature of Biochar and Activated Carbon from Pyrolysis-Activation of Vegetable (Lettuce) and Staple Food (Noodles) in Food Waste, *Resources, Conservation and Recycling Advances*, 2022, **15**, 200118.

23 M. Wilk, M. Śliz, K. Czerwińska and M. Śledź, The Effect of an Acid Catalyst on the Hydrothermal Carbonization of Sewage Sludge, *J. Environ. Manage.*, 2023, **345**, 118820.

24 S. Liu, G. Wu, L. Zhang, Y. Huang, J. Zhou and S. Zhang, Catalytic Pyrolysis of Pine Sawdust over Activated Carbon-Supported Fe for Phenol-Rich Bio-Oil, *J. Anal. Appl. Pyrolysis*, 2023, **171**, 105959, DOI: 10.1016/j.jaap.2023.105959.

25 D. Duan, D. Chen, L. Huang, Y. Zhang, Y. Zhang, Q. Wang, G. Xiao, W. Zhang, H. Lei and R. Ruan, Activated Carbon from Lignocellulosic Biomass as Catalyst: A Review of the Applications in Fast Pyrolysis Process, *J. Anal. Appl. Pyrolysis*, 2021, **158**, 105246, DOI: 10.1016/j.jaap.2021.105246.

26 S. Kim, Y. Lee, K. Y. Andrew Lin, E. Hong, E. E. Kwon and J. Lee, The Valorization of Food Waste via Pyrolysis, *J. Cleaner Prod.*, 2020, **259**, 120816, DOI: 10.1016/j.jclepro.2020.120816.

27 S. V. Qaramaleki, Á. F. Mohedano and C. J. Coronella, Phosphorus Recovery from Aqueous Product of Hydrothermal Carbonization of Cow Manure, *Waste Manage.*, 2023, **168**, 301–310, DOI: 10.1016/j.wasman.2023.06.013.

28 A. L. Pauline and K. Joseph, Hydrothermal Carbonization of Organic Wastes to Carbonaceous Solid Fuel – A Review of Mechanisms and Process Parameters, *Fuel*, 2020, **279**, 118472, DOI: 10.1016/j.fuel.2020.118472.

29 G. Yadav, N. Yadav and M. Ahmaruzzaman, Advances in Biomass Derived Low-Cost Carbon Catalyst for Biodiesel Production: Preparation Methods, Reaction Conditions, and Mechanisms, *RSC Adv.*, 2023, 23197–23210.

30 W. Mateo, H. Lei, E. Villota, M. Qian, Y. Zhao, E. Huo, Q. Zhang, X. Lin and C. Wang, One-Step Synthesis of Biomass-Based Sulfonated Carbon Catalyst by Direct Carbonization-Sulfonation for Organosolv Delignification, *Bioresour. Technol.*, 2021, **319**, 124194.

31 M. El Saied, A. M. A. El Naggar, F. I. Elhosiny and F. Y. El kady, A Comprehensive Investigation on Biomass Solid Waste Conversion to a Novel Catalyst for Hydrothermal Production of Bio-Fuel Feedstock, *J. Cleaner Prod.*, 2019, **218**, 157–166, DOI: **10.1016/j.jclepro.2019.01.320**.

32 Y. Shen, A Review on Hydrothermal Carbonization of Biomass and Plastic Wastes to Energy Products, *Biomass Bioenergy*, 2020, **134**, 105479, DOI: **10.1016/j.biombioe.2020.105479**.

33 M. Retajczyk, A. Wróblewska, A. Szymańska and B. Michalkiewicz, Isomerization of Limonene over Natural Zeolite-Clinoptilolite, *Clay Miner.*, 2019, **54**(2), 121–129, DOI: **10.1180/clm.2019.18**.

34 C. P. Tavera Ruiz, P. Gauthier-Maradei, M. Capron, C. Pirez, O. Gardoll, B. Katryniok and F. Dumeignil, Transformation of Dl Limonene into Aromatic Compounds Using Supported Heteropolyacid Catalysts, *Catal. Lett.*, 2019, **149**(1), 328–337, DOI: **10.1007/S10562-018-2606-Y**.

35 D. Makarouni, S. Lycourghiotis, E. Kordouli, K. Bourikas, C. Kordulis and V. Dourtoglou, Transformation of Limonene into P-Cymene over Acid Activated Natural Mordenite Utilizing Atmospheric Oxygen as a Green Oxidant: A Novel Mechanism, *Appl. Catal., B*, 2018, **224**, 740–750, DOI: **10.1016/J.APCATB.2017.11.006**.

36 L. Patrylak, S. Zubenko, S. Konovalov, A. Yakovenko, V. Povazhnyi, O. Pertko, Y. Voloshyna, O. Melnychuk and M. Filonenko, Isomerization of Limonene on Zeolite-Containing Catalysts Based on Kaolin, *Chem. J. Mold.*, 2022, **17**(2), 84–93, DOI: **10.19261/CJM.2022.980**.

37 G. L. K. Hunter and W. B. Brogden, Isomerization and Disproportionation of D-Limonene on Silica Gel, *J. Org. Chem.*, 1963, **28**(6), 1679–1682, DOI: **10.1021/jo01041a063**.

38 M. Retajczyk and A. Wróblewska, The Isomerization of Limonene over the Ti-SBA-15 Catalyst—the Influence of Reaction Time, Temperature, and Catalyst Content, *Catalysts*, 2017, **7**(9), 273.

39 S. Lycourghiotis, D. Makarouni, E. Kordouli, K. Bourikas, C. Kordulis and V. Dourtoglou, Activation of Natural Mordenite by Various Acids: Characterization and Evaluation in the Transformation of Limonene into p-Cymene, *Mol. Catal.*, 2018, **450**, 95–103, DOI: **10.1016/j.mcat.2018.03.013**.

40 I. Thushari, S. Babel and C. Samart, Biodiesel Production in an Autoclave Reactor Using Waste Palm Oil and Coconut Coir Husk Derived Catalyst, *Renewable Energy*, 2019, 125–134, DOI: **10.1016/j.renene.2018.11.030**.

41 C. E. Bounoukta, C. Megías-Sayago, S. Ivanova, A. Penkova, F. Ammari, M. A. Centeno and J. A. Odriozola, Effect of the Sulphonating Agent on the Catalytic Behavior of Activated Carbons in the Dehydration Reaction of Fructose in DMSO, *Appl. Catal., A*, 2021, **617**, 118108.

42 S. P. De Matos, H. F. Teixeira, Á. A. N. De Lima, V. F. Veiga-Junior and L. S. Koester, Essential Oils and Isolated Terpenes in Nanosystems Designed for Topical Administration: A Review, *Biomolecules*, 2019, **9**(4), 138.

43 A. E. Harman-Ware, Conversion of Terpenes to Chemicals and Related Products, *Chem. Catal. Biomass Upgrading*, 2019, 529–568, DOI: **10.1002/9783527814794.ch13**.

44 G. T. T. Le, K. Arunaditya, J. Panichpol, T. Rodruangnon, S. Thongratkaew, K. Chaipojjana, K. Faungnawakij and T. Charinpanitkul, Sulfonated Magnetic Carbon Nanoparticles from Eucalyptus Oil as a Green and Sustainable Catalyst for Converting Fructose to 5-HMF, *Catal. Commun.*, 2021, **149**, 106229, DOI: **10.1016/j.catcom.2020.106229**.

45 E. G. Mission, A. T. Quitain, M. Sasaki and T. Kida, Synergizing Graphene Oxide with Microwave Irradiation for Efficient Cellulose Depolymerization into Glucose, *Green Chem.*, 2017, **19**(16), 3831–3843, DOI: **10.1039/c7gc01691c**.

46 K. Sheng, S. Zhang, J. Liu, S. E, C. Jin, Z. Xu and X. Zhang, Hydrothermal Carbonization of Cellulose and Xylan into Hydrochars and Application on Glucose Isomerization, *J. Cleaner Prod.*, 2019, **237**, 117831, DOI: **10.1016/j.jclepro.2019.117831**.

47 W. N. R. W. Isahak, M. W. M. Hisham and M. A. Yarmo, Highly Porous Carbon Materials from Biomass by Chemical and Carbonization Method: A Comparison Study, *J. Chem.*, 2013, DOI: **10.1155/2013/620346**.

48 P. Fernández, J. M. Fraile, E. García-Bordejé and E. Pires, Sulfonated Hydrothermal Carbons from Cellulose and Glucose as Catalysts for Glycerol Ketalization, *Catalysts*, 2019, **9**(10), 804, DOI: **10.3390/catal9100804**.

49 Z. Yao, W. Zhang and X. Yu, Fabricating Porous Carbon Materials by One-Step Hydrothermal Carbonization of Glucose, *Processes*, 2023, **11**(7), 1923, DOI: **10.3390/pr11071923**.

50 S. Thomas, *Understanding the Pearson Correlation Coefficient*, 2023, **https://articles.outlier.org/pearson-correlation-coefficient**.

51 Z. G. Gu, S. Grosjean, S. Bräse, C. Wöll and L. Heinke, Enantioselective Adsorption in Homochiral Metal-Organic Frameworks: The Pore Size Influence, *Chem. Commun.*, 2015, **51**(43), 8998–9001, DOI: **10.1039/c5cc02706c**.

52 R. S. Nunes, G. T. M. Xavier, A. L. Urzedo, P. S. Fadini, M. Romeiro, T. G. S. Guimarães, G. Labuto and W. A. Carvalho, Cleaner Production of Iron-Coated Quartz Sand Composites for Efficient Phosphorus Adsorption in Sanitary Wastewater : A Design of Experiments (DoE) Approach, *Sustainable Chem. Pharm.*, 2023, **35**, 101206, DOI: **10.1016/j.scp.2023.101206**.

53 M. Retajczyk, A. Wróblewska, A. Szymańska and B. Michalkiewicz, Isomerization of Limonene over Natural Zeolite-Clinoptilolite, *Clay Miner.*, 2019, **54**(2), 121–129, DOI: **10.1180/clm.2019.18**.

54 M. Retajczyk, A. Wróblewska, Z. C. Koren, B. Michalkiewicz, A. Szymańska and P. Miadlicki, Synthesis, Characterization, and Catalytic Applications of the Ti-Sba-16 Porous Material in the Selective and Green Isomerizations of Limonene and s-Carvone, *Catalysts*, 2020, **10**(12), 1–17, DOI: **10.3390/catal10121452**.

55 M. Retajczyk and A. Wróblewska, Isomerization and Dehydroaromatization of r(+)-Limonene over the Ti-Mcm-41 Catalyst: Effect of Temperature, Reaction Time and Catalyst Content on Product Yield, *Catalysts*, 2019, **9**(6), 508, DOI: **10.3390/catal9060508**.

56 G. M. Reis, L. F. L. Machado, R. S. Nunes, D. Mandelli and W. A. Carvalho, Tailored Sulfonated Carbons: Unraveling Enhanced Catalytic Dynamics for Fructose Dehydration under Conventional and Microwave Heating, *RSC Sustainability*, 2024, **2020**, 1456–1471, DOI: **10.1039/d4su00007b**.

57 S. Liu, Y. Zhu, Y. Liao, H. Wang, Q. Liu, L. Ma and C. Wang, Advances in Understanding the Humins: Formation, Prevention and Application, *Appl. Energy Combust. Sci.*, 2022, **10**, 100062, DOI: **10.1016/j.jaecs.2022.100062**.

58 A. W. W. Echtermeyer and J. Viell, Integrated Humin Formation and Separation Studied In Situ by Centrifugation, *ACS Omega*, 2024, **9**(6), 6432–6441, DOI: **10.1021/acsomega.3c06103**.

59 X. Fu, Y. Hu, P. Hu, H. Li, S. Xu, L. Zhu and C. Hu, Mapping out the Reaction Network of Humin Formation at the Initial Stage of Fructose Dehydration in Water, *Green Energy Environ.*, 2022, **9**(6), 1016–1026, DOI: **10.1016/j.gee.2022.09.012**.

60 Z. Xu, Y. Yang, P. Yan, Z. Xia, X. Liu and Z. C. Zhang, Mechanistic Understanding of Humin Formation in the Conversion of Glucose and Fructose to 5-Hydroxymethylfurfural in [BMIM]Cl Ionic Liquid, *RSC Adv.*, 2020, **10**(57), 34732–34737, DOI: **10.1039/d0ra05641c**.

61 L. Filiciotto, P. Tosi, A. M. Balu, E. de Jong, J. C. van der Waal, S. M. Osman, R. Luque and A. Mija, Humins as Bio-Based Template for the Synthesis of Alumina Foams, *Mol. Catal.*, 2022, **526**, 112363, DOI: **10.1016/j.mcat.2022.112363**.

62 Z. Cheng, J. L. Everhart, G. Tsilomelekis, V. Nikolakis, B. Saha and D. G. Vlachos, Structural Analysis of Humins Formed in the Brønsted Acid Catalyzed Dehydration of Fructose, *Green Chem.*, 2018, **20**(5), 997–1006, DOI: **10.1039/c7gc03054a**.

63 Y. Hu, H. Li, P. Hu, L. Li, D. Wu, Z. Xue, L. Zhu and C. Hu, Probing the Effects of Fructose Concentration on the Evolution of Humins during Fructose Dehydration, *React. Chem. Eng.*, 2022, **8**(1), 175–183, DOI: **10.1039/d2re00324d**.

64 S. K. R. Patil, J. Heltzel and C. R. F. Lund, Comparison of Structural Features of Humins Formed Catalytically from Glucose, Fructose, and 5-Hydroxymethylfurfuraldehyde, *Energy Fuels*, 2012, **26**, 5281–5293, DOI: **10.1021/ef3007454**.

65 C. Franz and J. Novak. *Sources of Essential Oils*; 2019.

66 W. He, S. Tashiro and M. Shionoya, Highly Selective Acid-Catalyzed Olefin Isomerization of Limonene to Terpinolene by Kinetic Suppression of Overreactions in a Confined Space of Porous Metal-Macrocycle Frameworks, *Chem. Sci.*, 2022, **13**(30), 8752–8758, DOI: **10.1039/d2sc01561g**.